PERGAMON

Available online at www.sciencedirect.com
SCIENCE DIRECT®

Polyhedron 22 (2003) 199–203

POLYHEDRON

www.elsevier.com/locate/poly

Synthesis and structure of $[\mathrm{pz}^{\mathrm{Bu}^t_2}]\mathrm{Mo(PMe_3)_4H}$, a d^4 molybdenum complex that exhibits η^2-coordination of the 3,5-di-*t*-butylpyrazolyl ligand

Guang Zhu, Joseph M. Tanski, Gerard Parkin *

Department of Chemistry, Columbia University, New York, NY 10027, USA

Received 14 August 2002; accepted 30 September 2002

Abstract

$\mathrm{Mo(PMe_3)_6}$ reacts with $[\mathrm{pz}^{\mathrm{Bu}^t_2}]\mathrm{H}$ at 80 °C to give $[\eta^2\text{-}\mathrm{pz}^{\mathrm{Bu}^t_2}]\mathrm{Mo(PMe_3)_4H}$, the first structurally characterized d^4 η^2-pyrazolyl complex of molybdenum. The hydride ligand of $[\eta^2\text{-}\mathrm{pz}^{\mathrm{Bu}^t_2}]\mathrm{Mo(PMe_3)_4H}$ is displaced from the mean $\mathrm{Mo{-}N{-}N{-}P_{\mathit{cis}}{-}P_{\mathit{cis}}}$ plane, such that the distorted seven-coordinate geometry may be viewed as being based on a distorted dodecahedron with a vacant coordination site. DFT (B3LYP) calculations suggest that the origin of the displacement of the hydride ligand is due to steric interactions with the pair of '*cis*' $\mathrm{PMe_3}$ ligands.

Keywords: 3,5-Di-*t*-butylpyrazolyl; Molybdenum complexes; $[\mathrm{pz}^{\mathrm{Bu}^t_2}]\mathrm{Mo(PMe_3)_4H}$; η^2-Coordination; $\mathrm{Mo(PMe_3)_6}$

1. Introduction

As part of our studies concerned with modeling aspects of hydrodenitrogenation (HDN), the process by which nitrogen is removed from fossil fuels [1], we have investigated the reactivity of $\mathrm{Mo(PMe_3)_6}$ towards a variety of heterocycles containing a single nitrogen atom, such as pyrrole, indole, carbazole, pyridine, quinoline and acridine [2]. In this paper, we describe the reactivity of $\mathrm{Mo(PMe_3)_6}$ towards a heterocycle containing two nitrogen atoms, namely 3,5-di-*tert*-butylpyrazole ($[\mathrm{pz}^{\mathrm{Bu}^t_2}]\mathrm{H}$).

2. Results and discussion

Although the coordination chemistry of pyrazoles has been widely studied [3], it is surprising that very few molybdenum–pyrazolyl complexes have been isolated. For example, the only structurally characterized mononuclear molybdenum–pyrazolyl complexes of which we are aware are d^2 $\mathrm{Cp_2Mo(\eta^1\text{-}pz)_2}$ [4] and d^0 $[\eta^2\text{-}\mathrm{pz}^{\mathrm{Bu}^t_2}]\mathrm{Mo(O)_2Cl}$ [5,6]. It is, therefore, significant that $\mathrm{Mo(PMe_3)_6}$ reacts with $[\mathrm{pz}^{\mathrm{Bu}^t_2}]\mathrm{H}$ at 80 °C to give the d^4 pyrazolyl complex $[\eta^2\text{-}\mathrm{pz}^{\mathrm{Bu}^t_2}]\mathrm{Mo(PMe_3)_4H}$ (Scheme 1). The molecular structure of $[\eta^2\text{-}\mathrm{pz}^{\mathrm{Bu}^t_2}]\mathrm{Mo(PMe_3)_4H}$ has been determined by X-ray diffraction, as illustrated in Figs. 1 and 2. Selected bond lengths and angles are listed in Table 1.

The most significant feature of the structure of $[\eta^2\text{-}\mathrm{pz}^{\mathrm{Bu}^t_2}]\mathrm{Mo(PMe_3)_4H}$ is that the pyrazolyl ligand coordinates in an uncommon η^2-manner for molybdenum [5,7]. Indeed, it is only in recent years that this coordination mode has become extensively studied for transition metals [8,9]. With a d^4 configuration, the structure of $[\eta^2\text{-}\mathrm{pz}^{\mathrm{Bu}^t_2}]\mathrm{Mo(PMe_3)_4H}$ is also of interest because it has been noted that the η^2-coordination mode of pyrazolyl ligands is not typically observed for metals with $d^{\geq 2}$ configurations [8e]. In this regard, the Mo–N bond length of $[\eta^2\text{-}\mathrm{pz}^{\mathrm{Bu}^t_2}]\mathrm{Mo(PMe_3)_4H}$ (2.26 Å) is greater than that of the d^0 complex $[\eta^2\text{-}\mathrm{pz}^{\mathrm{Bu}^t_2}]\mathrm{Mo(O)_2Cl}$ (2.07 Å) [5], it is also longer than the Mo–N bond of $\mathrm{Cp_2Mo(\eta^1\text{-}pz)_2}$ (2.16 Å) [4], in which the pyrazolyl ligand coordinates in an η^1-manner.

The η^2-coordination mode for the pyrazolyl ligand in this system also provides an interesting contrast with the

---

* Corresponding author. Tel.: +1-212-932-1289; fax: +1-212-854-2202

E-mail address: parkin@chem.columbia.edu (G. Parkin).

0277-5387/02/$ - see front matter © 2002 Elsevier Science Ltd. All rights reserved.
PII: S0277-5387(02)01265-2

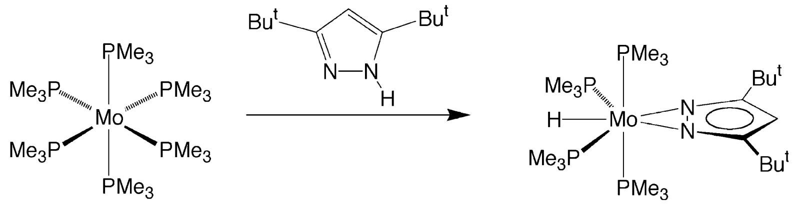

Scheme 1.

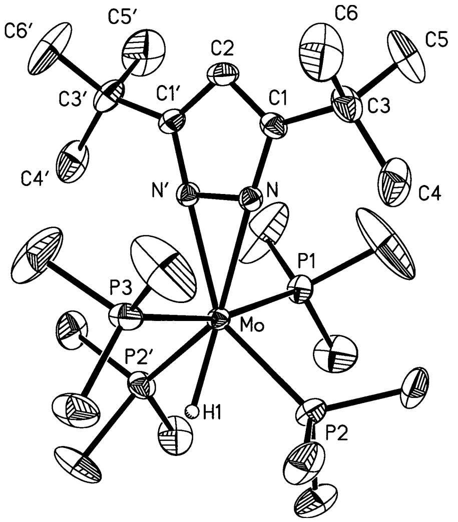

Fig. 1. Molecular structure of $[\eta^2\text{-pz}^{\text{Bu}^t_2}]\text{Mo(PMe}_3)_4\text{H}$.

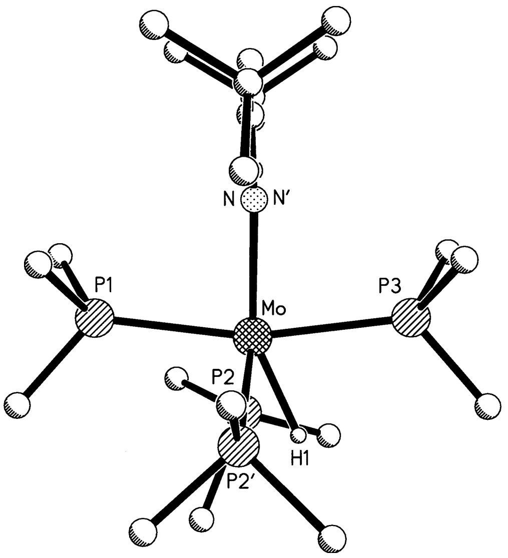

Fig. 2. Illustration of the asymmetric location of the hydride ligand.

η^5-coordination observed for the pyrrolyl derivative, $(\eta^5\text{-pyr})\text{Mo(PMe}_3)_3\text{H}$, obtained from the corresponding reaction of $\text{Mo(PMe}_3)_6$ with pyrrole [2]. The η^2-pyrazolyl coordination mode is, nevertheless, similar to that of the related η^2-pyridyl complex, $[\eta^2\text{-(C}_5\text{H}_4\text{N)]Mo(PMe}_3)_4\text{H}$ [2].

Table 1
Selected bond lengths (Å) and angles (°) for $[\eta^2\text{-pz}^{\text{Bu}^t_2}]\text{Mo(PMe}_3)_4\text{H}$

Bond lengths			
Mo–N	2.260(2)	Mo–P(1)	2.465(1)
Mo–P(2)	2.375(1)	Mo–P(3)	2.468(1)
Mo–H	1.70(4)	N–N′	1.371(4)
Bond angles			
N–Mo–N′	35.3(1)	N–Mo–P(1)	84.43(6)
N–Mo–P(2)	109.67(5)	N–Mo–P(3)	82.49(6)
P(1)–Mo–P(2)	89.78(3)	P(1)–Mo–P(3)	166.26(4)
P(2)–Mo–P(3)	98.54(3)	P(2)–Mo–P(2′)	104.93(5)

The X-ray structure indicates that there are two classes of PMe_3 ligands, namely a '*trans*' pair [P(1)–Mo–P(3) = 166.26(4)°] that are displaced slightly towards the pyrazolyl ligand, and a '*cis*' pair that resides in the Mo–pyrazolyl plane and are displaced towards the hydride ligand [P(2)–Mo–P(2′) = 104.93(5)°]. Notably, the hydride ligand does not lie in the Mo–N–N–P_{cis}–P_{cis} plane, but is displaced from the *pseudo*-C_2 axis, such that the distorted seven-coordinate geometry may be viewed as being based on a dodecahedron with a vacant coordination site. We have performed DFT (B3LYP) calculations to address the origin for the asymmetric placement of the hydride ligand. Geometry optimization of $[\eta^2\text{-pz}^{\text{Bu}^t_2}]\text{Mo(PMe}_3)_4\text{H}$ resulted in a structure (Fig. 3) which is very similar to that determined experimentally (Table 2). The magnitude of the stabilization afforded by the displacement of the hydride ligand from the mean Mo–N–N–P_{cis}–P_{cis} plane was determined by performing a calculation on a structure in which the hydride ligand was constrained to lie in the Mo–N–N–P_{cis}–P_{cis} plane. Notably, the geometry optimized constrained structure was observed to be 4.4 kcal mol^{-1} higher in energy than that with the hydride ligand displaced from the Mo–N–N–P_{cis}–P_{cis} plane. Comparison of the constrained and unconstrained structures suggests a steric explanation for the displacement of the hydride ligand. Specifically, such displacement relieves steric interactions between the hydride ligand and the two *cis*-phosphine ligands. Evidence, which supports this notion, is provided by a complementary study on hypothetical $[\eta^2\text{-pz}]\text{Mo(PH}_3)_4\text{H}$, in which the *t*-butyl and methyl groups were replaced by hydrogen. The structures of the freely geometry optimized and constrained structures are illustrated in Fig. 4, and compare favorably with those of $[\eta^2\text{-pz}^{\text{Bu}^t_2}]\text{Mo(PMe}_3)_4\text{H}$ (Fig. 3 and Table 1). However, the difference in energy between the two structures of $[\eta^2\text{-pz}]\text{Mo(PH}_3)_4\text{H}$

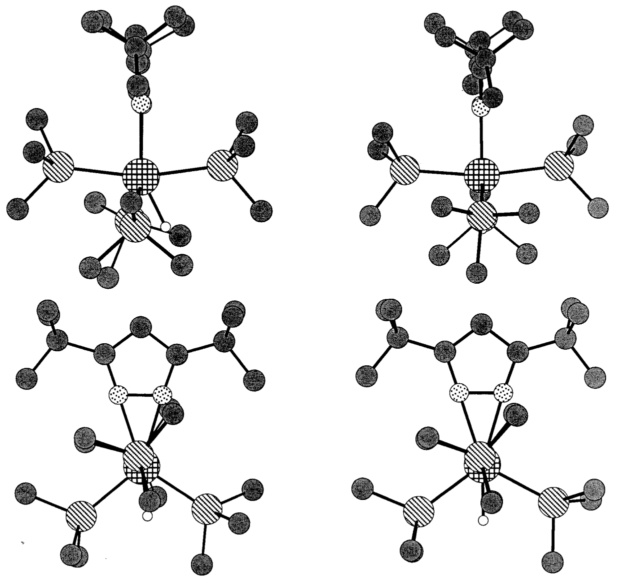
(a)
geometry optimized with
no constraints

(b)
geometry optimized
constraining Mo–H–N–N–P–P
to lie in a plane
(H^{SCF}_{rel} = 4.4 kcal mol^{-1})

Fig. 3. Comparison of the geometry optimized structure of $[\eta^2\text{-pz}^{Bu^t_2}]Mo(PMe_3)_4H$: (a) without constraints and (b) with the hydride ligand constrained to lying in the Mo–N–N–P_{cis}–P_{cis} plane.

Table 2
Selected bond lengths (Å) and angles (°) for geometry optimized $[\eta^2\text{-pz}^{Bu^t_2}]Mo(PMe_3)_4H$, $[\eta^2\text{-pz}]Mo(PMe_3)_4H$ and $[\eta^2\text{-pz}]Mo(PH_3)_4H$

	$[\eta^2\text{-pz}^{Bu^t_2}]$-$Mo(PMe_3)_4H$ [a]	$[\eta^2\text{-pz}]$-$Mo(PMe_3)_4H$	$[\eta^2\text{-pz}]$-$Mo(PH_3)_4H$
Bond lengths			
Mo–$P_{'trans'(av)}$	2.52 [2.47 Å]	2.51	2.46
Mo–$P_{'cis'(av)}$	2.44 [2.38 Å]	2.42	2.41
Mo–N_{av}	2.32 [2.26 Å]	2.29	2.23
Mo–H	1.71 [1.70 Å]	1.72	1.72
Bond angles			
$P_{'trans'}$–Mo–$P_{'trans'}$	164.6 [166.3°]	164.8	173.7
$P_{'cis'}$–Mo–$P_{'cis'}$	106.3 [104.9°]	114.0	120.7

[a] Experimental values in brackets.

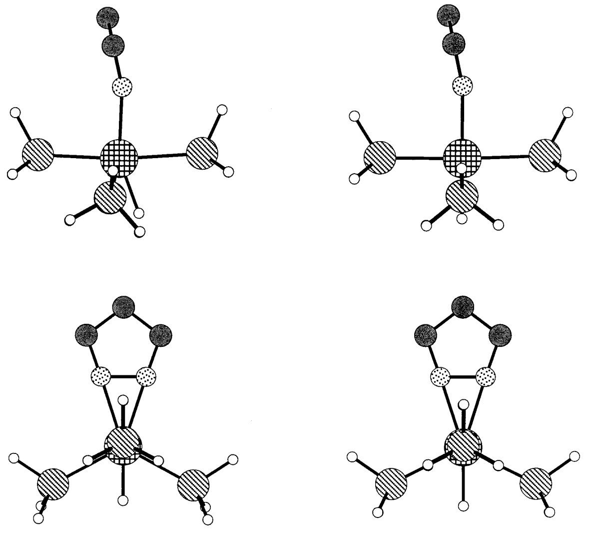
(a)
geometry optimized with
no constraints

(b)
geometry optimized
constraining Mo–H–N–N–P–P
to lie in a plane
(H^{SCF}_{rel} = 1.5 kcal mol^{-1})

Fig. 4. Comparison of the geometry optimized structure of $[\eta^2\text{-pz}]Mo(PH_3)_4H$: (a) without constraints and (b) with the hydride ligand constrained to lying in the Mo–N–N–P_{cis}–P_{cis} plane.

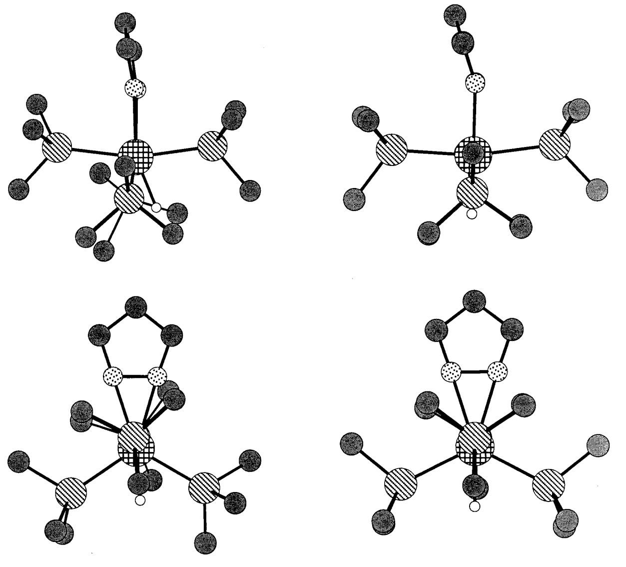
(a)
geometry optimized with
no constraints

(b)
geometry optimized
constraining Mo–H–N–N–P–P
to lie in a plane
(H^{SCF}_{rel} = 1.2 kcal mol^{-1})

Fig. 5. Comparison of the geometry optimized structure of $[\eta^2\text{-pz}]Mo(PMe_3)_4H$: (a) without constraints and (b) with the hydride ligand constrained to lying in the Mo–N–N–P_{cis}–P_{cis} plane.

(1.5 kcal mol^{-1}) is less than those for $[\eta^2\text{-pz}^{Bu^t_2}]Mo(PMe_3)_4H$ (4.4 kcal mol^{-1}) since the steric interactions are reduced.

We have also performed calculations on the hybrid system $[\eta^2\text{-pz}]Mo(PMe_3)_4H$ in which only the *t*-butyl groups of the pyrazolyl ligand are removed. In accord with the calculated structures of $[\eta^2\text{-pz}^{Bu^t_2}]Mo(PMe_3)_4H$ and $[\eta^2\text{-pz}]Mo(PH_3)_4H$, the structure of $[\eta^2\text{-pz}]Mo(PMe_3)_4H$ with the hydride ligand displaced from the Mo–N–N–P_{cis}–P_{cis} plane is also lower in energy by 1.2 kcal mol^{-1} (Fig. 5). Interestingly, however, the difference in energy for $[\eta^2\text{-pz}]Mo(PMe_3)_4H$ is less than that for $[\eta^2\text{-pz}^{Bu^t_2}]Mo(PMe_3)_4H$, indicating that the substituents on the pyrazolyl ligand also influence the relative stability. Comparison of the structures of $[\eta^2\text{-pz}]Mo(PMe_3)_4H$ and $[\eta^2\text{-pz}^{Bu^t_2}]Mo(PMe_3)_4H$ demonstrates that removal of the *t*-butyl groups on the pyrazolyl ligand allows the angle between the '*cis*' PMe_3 ligands to expand from 106.3° to 114.0° in the unconstrained structures, and from 115.2° to 125.2° in the constrained structures. This increase in the '*cis*' P–Mo–P bond angle from $[\eta^2\text{-pz}^{\mathrm{Bu}^t_2}]\mathrm{Mo(PMe_3)_4H}$ to $[\eta^2\text{-pz}]\mathrm{Mo(PMe_3)_4H}$ would be expected to facilitate the placement of the hydride ligand on the *pseudo*-C_2 axis of the latter molecule.

Since the energy of the structure of $[\eta^2\text{-pz}^{\mathrm{Bu}^t_2}]\mathrm{Mo(PMe_3)_4H}$ with the hydride ligand constrained to lying in the $\mathrm{Mo{-}N{-}N{-}P_{\mathit{cis}}{-}P_{\mathit{cis}}}$ plane is only 4.4 kcal mol^{-1} higher in energy than the unconstrained structure, it is evident that there should not be a large barrier for inversion of the hydride ligand. In accord with this proposal, the molecule is fluxional on the NMR time-scale. Thus, the hydride ligand is characterized by a triplet of triplets resonance at δ −6.98 ppm [$^2J_{\mathrm{P-H}} = 28$ and 86 Hz] in the ^{1}H NMR spectrum due to coupling to two different pairs of PMe_3 ligands, rather than a doublet of doublet of triplets that would be predicted for the asymmetric static structure.

3. Summary

In conclusion, the first structurally characterized d^4 η^2-pyrazolyl complex of molybdenum, namely $[\eta^2\text{-pz}^{\mathrm{Bu}^t_2}]\mathrm{Mo(PMe_3)_4H}$, has been obtained by the reaction of $\mathrm{Mo(PMe_3)_6}$ with $[\mathrm{pz}^{\mathrm{Bu}^t_2}]\mathrm{H}$. The structure of $[\eta^2\text{-pz}^{\mathrm{Bu}^t_2}]\mathrm{Mo(PMe_3)_4H}$ is of particular note because η^2-coordination of pyrazolyl ligands is not typically observed for metals with $d^{\geq 2}$ configurations.

4. Experimental

4.1. General considerations

All manipulations were performed using a combination of glovebox, high vacuum, and Schlenk techniques under an argon atmosphere. Solvents were purified and degassed by standard procedures. $\mathrm{Mo(PMe_3)_6}$ [10] and 3,5-di(*t*-butyl)pyrazole [11] were prepared by literature methods. Benzene-d_6 was obtained from Cambridge Isotopes and dried over 4 Å molecular sieves prior to use. ^{1}H and ^{13}C NMR spectra were measured on Bruker 300 DRX, Bruker Avance 400 DRX, and Bruker Avance 500 DMX spectrometers. Chemical shifts are reported in ppm relative to $SiMe_4$ ($\delta = 0$) and were referenced internally with respect to the protio solvent impurity ($\delta = 7.15$ for C_6D_5H) and the ^{13}C resonance ($\delta = 128.0$ for C_6D_6), respectively. ^{31}P NMR spectra were referenced relative to 85% H_3PO_4 ($\delta = 0$) using $P(OMe)_3$ as an external reference ($\delta = 141.0$). All coupling constants are reported in hertz. IR spectra were recorded on a Perkin–Elmer Paragon 1000 spectrophotometer.

4.2. Synthesis of $[\eta^2\text{-pz}^{\mathrm{Bu}^t_2}]\mathrm{Mo(PMe_3)_4H}$

A mixture of $\mathrm{Mo(PMe_3)_6}$ (77 mg, 0.14 mmol) and 2,5-di-*tert*-butylpyrazole (25 mg, 0.14 mmol) in benzene (ca. 1 ml) was heated at 80 °C for 20 h, after which period the volatile components were removed in vacuo. The residue was extracted into benzene, filtered, and the filtrate was lyophilized to give $[\eta^2\text{-pz}^{\mathrm{Bu}^t_2}]\mathrm{Mo(PMe_3)_4H}$ as a dark brown solid (79 mg, 98% yield). ^{1}H NMR (C_6D_6): −6.98 [tt, $^2J_{\mathrm{P-H}} = 28$, $^2J_{\mathrm{P-H}} = 86$, 1H of $\mathrm{Mo\underline{H}}$], 0.93 [s, 18H of $\mathrm{Mo(P(CH_3)_3)_4}$], 1.47 [br, 18H of $\mathrm{Mo(P(CH_3)_3)_4}$ and 18 H of $\mathrm{2C(CH_3)_3}$], 5.88 [s, 1H of $\mathrm{NCC\underline{H}CN}$]. ^{13}C NMR ($C_6D_6$): 22.7 [t, $^1J_{\mathrm{P-C}} = 7$, 6C of $\mathrm{Mo(P(\underline{C}H_3)_3)_4}$], 31.4 [dt, $^1J_{\mathrm{P-C}} = 19$, $^3J_{\mathrm{P-C}} = 8$, 6C of $\mathrm{Mo(P(\underline{C}H_3)_3)_4}$], 32.1 [s, 6C of $\mathrm{2C(\underline{C}H_3)_3}$], 32.4 [s, 2C of $\mathrm{2\underline{C}(CH_3)_3}$], 98.2 [s, 1C of $\mathrm{NC\underline{C}HCN}$], 158.1 [s, 2C of $\mathrm{N\underline{C}CH\underline{C}N}$]. ^{31}P NMR ($C_6D_6$): 3.2 [t, $^2J_{\mathrm{P-P}} = 26$, 2P of $\mathrm{Mo(\underline{P}(CH_3)_3)_4}$], 27.6 [t, $^2J_{\mathrm{P-P}} = 26$, 2P of $\mathrm{Mo(\underline{P}(CH_3)_3)_4}$]. IR Data (KBr disk, cm^{-1}): 3234 (w), 3101 (w), 2961 (vs), 2900 (vs), 2800 (m), 1832 (w), 1569 (w), 1505 (m), 1457 (m), 1422 (s), 1358 (s), 1324 (w), 1289 (s), 1269 (s), 1250 (m), 1218 (m), 1129 (w), 1010 (m), 930 (vs), 843 (s), 805 (m), 758 (m), 704 (s), 651 (s), 516 (w), 463 (w).

4.3. X-ray structure determination

Crystals suitable for X-ray diffraction study were grown from benzene by slow evaporation. X-ray diffraction data were collected on a Bruker P4 diffractometer equipped with a SMART CCD detector and crystal data, data collection and refinement parameters

Table 3
Crystal, intensity collection and refinement data for $[\eta^2\text{-pz}^{\mathrm{Bu}^t_2}]\mathrm{Mo(PMe_3)_4H}$

Lattice	orthorhombic
Formula	$C_{23}H_{56}N_2P_4Mo$
Formula weight	580.52
Space group	*Pnma*
a (Å)	18.950(2)
b (Å)	17.355(2)
c (Å)	9.895(1)
α (°)	90
β (°)	90
γ (°)	90
V (Å^3)	3254(1)
Z	4
Temperature (K)	243
Radiation λ (Å)	0.71073
$\rho_{\mathrm{calc.}}$ (g cm^{-3})	1.185
μ Mo Kα (mm^{-1})	0.612
θ Max (°)	28.1
Number of data	3894
Number of parameters	181
R_1	0.0392
wR_2	0.1344
Goodness-of-fit	1.000

are summarized in Table 3. The structures were solved using direct methods and standard difference map techniques, and were refined by full-matrix least-squares procedures on F^2 with SHELXTL (Version 5.03) [12].

4.4. Computational details

All calculations were carried out using DFT as implemented in the Jaguar 4.1 suite [13] of ab initio quantum chemistry programs. Geometry optimizations were performed with the B3LYP functional and the 6-31G** basis set for C, H, N and P, while Mo was represented using the Los Alamos LACVP** basis set that includes relativistic effective core potentials. The energies of the optimized structures were reevaluated by additional single point calculations on each optimized geometry using the cc-pVTZ(-f) correlation consistent triple-ζ basis set cc-pVTZ(-f) for C, H, N, and P, and LACV3P** for Mo.

5. Supplementary material

Crystallographic data for the structural analysis have been deposited with the Cambridge Crystallographic Data Centre, CCDC No. 190998 for $[\eta^2\text{-pz}^{\mathrm{Bu}^t_2}]\mathrm{Mo}(\mathrm{PMe}_3)_4\mathrm{H}$. Copies of this information may be obtained free of charge from The Director, CCDC, 12 Union Road, Cambridge, CB2 1EZ, UK (fax: +44-1223-336033; e-mail: deposit@ccdc.cam.ac.uk or www: http://www.ccdc.cam.ac.uk).

Acknowledgements

We thank the US Department of Energy, Office of Basic Energy Sciences (DE-FG02-93ER14339) for support of this research.

References

[1] (a) R.J. Angelici, Polyhedron 16 (1997) 3073;
(b) K.J. Weller, P.A. Fox, S.D. Gray, D.E. Wigley, Polyhedron 16 (1997) 3139;
(c) C. Bianchini, A. Meli, F. Vizza, Eur. J. Inorg. Chem. (2001) 43;
(d) R.M. Laine, Catal. Rev.-Sci. Eng. 25 (1983) 459;
(e) J.G. Reynolds, Chem. Ind. (1991) 570.

[2] G. Zhu, J.M. Tanski, D.G. Churchill, K.E. Janak, G. Parkin, J. Am. Chem. Soc. 124 (2002) 13658.

[3] (a) A.P. Sadimenko, Adv. Heterocyclic Chem. 80 (2001) 157;
(b) A.P. Sadimenko, S.S. Basson, Coord. Chem. Rev. 147 (1996) 247;
(c) S. Trofimenko, Chem. Rev. 72 (1972) 497.

[4] M.A.A.F.D.C.T. Carrondo, A.M.T.S. Domingos, J. Organomet. Chem. 253 (1983) 53.

[5] K. Most, S. Köpke, F. Dall'Antonia, N.C. Mösch-Zanetti, Chem. Commun. (2002) 1676.

[6] For some bridging pyrazolyl complexes, see: (a) M.J. Calhorda, A.R. Dias, J. Organomet. Chem. 197 (1980) 291. (b) J.C. Weis, W. Beck, Chem. Ber. 105 (1972) 3203.

[7] The complex $[\mathrm{AsPh}_4]\{\mathrm{Mo(CO)}_4[\eta^2\text{–pz}]\}$ has been reported, but was not characterized by X-ray diffraction (see Ref. [6b]).

[8] See, for example: (a) J.E. Cosgriff, G.B. Deacon, Angew. Chem. Int. Ed. 37 (1998) 286. (b) I.A. Guzei, A.G. Baboul, G.P.A. Yap, A.L. Rheingold, H.B. Schlegel, C.H. Winter, J. Am. Chem. Soc. 119 (1997) 3387. (c) I.A. Guzei, G.P.A. Yap, C.H. Winter, Inorg. Chem. 36 (1997) 1738. (d) D. Röttger, G. Erker, M. Grehl, R. Fröhlich, Organometallics 13 (1994) 3897. (e) K.R. Gust, J.E. Knox, M.J. Heeg, H.B. Schlegel, C.H. Winter, Angew. Chem. Int. Ed. 41 (2002) 1591. (f) K.R. Gust, M.J. Heeg, C.H. Winter, Polyhedron 20 (2001) 805. (g) C. Yélamos, M.J. Heeg, C.H. Winter, Inorg. Chem. 38 (1999) 1871. (h) C. Yélamos, M.J. Heeg, C.H. Winter, Organometallics 18 (1999) 1168.

[9] η^5-Pyrazolyl complexes have also been recently obtained. See: J.R. Perera, M.J. Heeg, H.B. Schlegel, C.H. Winter, J. Am. Chem. Soc. 121 (1999) 4536.

[10] V.J. Murphy, G. Parkin, J. Am. Chem. Soc. 117 (1995) 3522.

[11] J. Elguero, E. Gonzalez, R. Jacquier, Bull. Soc. Chim. Fr. (1968), 707.

[12] G.M. Sheldrick, SHELXTL, An Integrated System for Solving, Refining and Displaying Crystal Structures from Diffraction Data, University of Göttingen, Göttingen, Germany, 1981.

[13] Jaguar 4.1, Schrödinger, Inc., Portland, OR, 2001.